Real-Time Detection and Repair of Cycle-Slip Based on Pseudo-range Phase Combinations for Un-differenced GNSS Triple-Frequency Observations

Lingdong Meng, Junping Chen, Jiexian Wang and Yize Zhang

Abstract For the detection and repair of cycle-slip for un-differenced GNSS triple-frequency observations, current algorithms have difficulties in efficiency, stability and even some special cycle-slip combinations cannot be detected. This paper investigates the strategies in real-time detection and repair of cycle-slip. Geometry free ionospheric free code-phase combinations together with phase combinations are used, where the selection criteria of combination coefficients is based on the principle of the minimal condition number. Advantage of the method is that each cycle-slip value can be calculated without searching, thus the efficiency is improved and success rate is still high. Experiment results show that even under the severe ionospheric conditions, cycle-slips of triple-frequency un-differenced observations can be detected and repaired.

Keywords Un-differenced triple-frequency observations · Cycle-slip detection and repair · Code-phase combination

1 Introduction

Triple frequency data can form more combinations with longer wavelength, smaller noise and less affected by ionosphere, which is useful for cycle-slip detection [1] and integer ambiguity solution [2]. There have been many algorithms to detect and repair cycle-slips [3]. The high order-difference method is intuitive but it is difficult to realize in source coding [4]; Extrapolation method based on gray theory [5] cannot work well in carrier with irregular motion and when cycle-slip happened in

L. Meng · J. Wang
College of Surveying and Geo-Informatics, Tongji University, Shanghai 200092, China

J. Chen (✉) · Y. Zhang
Shanghai Astronomical Observatory Chinese Academy of Sciences, Shanghai 200030, China
e-mail: junping@shao.ac.cn

J. Chen
University of Chinese Academy of Sciences, Beijing 100049, China

J. Sun et al. (eds.), *China Satellite Navigation Conference (CSNC) 2018 Proceedings*, Lecture Notes in Electrical Engineering 498,
https://doi.org/10.1007/978-981-13-0014-1_57

the first few epochs; Triple-frequency TurboEdit cycle-slip processing method using searching way to calculate the value of each frequency [6] cycle-slips is of low efficiency, unstable and complicated; The influence of ionosphere is not fully considered in the method based on code-phase combinations for triple-frequency un-differenced observations [1]; The method of Geometry Free Ionospheric Free (GFIF) combinations united the real-time estimation of ionospheric variation delay [7] can overcome the effect of ionospheric delay but this method is too complicated with huge processing burden.

In this paper, the triple-frequency GFIF code combinations are based on the criteria of less pseudo-range noise. Phase combinations used in this paper is selected with the criteria of less ionosphere delay effects and noise. The principle of the minimal conditions of coefficient matrix are implemented for the definition of the equation to be used in the calculation of cycle-slip. Finally, the method of this paper is verified using the BDS and GPS triple-frequency observations of IGS.

2 The Cycle-Slip Detection Observations

2.1 Triple-Frequency GFIF Code-Phase Combination

Referred to the idea of dual-frequency MW combination, triple-frequency GFIF combinations can eliminate the geometric distance-related terms and the first order effects of ionospheric delay. The pseudo-range and phase observation equation can be shown as Eqs. (1) and (2) respectively.

$$P_i = \rho + \frac{f_1^2}{f_i^2} I + \varepsilon_{p_i} \tag{1}$$

$$\varphi_i = \frac{\rho}{\lambda_i} + N_i - \frac{f_1^2}{f_i^2} I' + \varepsilon_{\varphi_i} \tag{2}$$

where, P and φ is the raw pseudo-range and phase observation; ρ is the geometric distance between satellite and receiver antennas including the satellite clock error and tropospheric delay; I and I' are the ionospheric group delay on the first frequency in meters and ionospheric phase delay on the first frequency in cycles respectively; ε_{φ_i} and ε_{p_i} are the receiver code noise in meters and the receiver phase noise in cycles respectively; i refers to frequency number. According to Eqs. (1) and (2), the integer ambiguity can be calculated as Eq. (3).

$$N = aN_1 + bN_2 + cN_3 = a\varphi_1 + b\varphi_2 + c\varphi_3 - \frac{(lP_1 + mP_2 + nP_3)}{\lambda} \tag{3}$$

In Eq. (3), to keep the integer features of ambiguity, a, b and c must be integer, while l, m and n can be real number.

According to the [6], the GFIF code-phase combination coefficients follows the Eqs. (4) and (5).

$$l + m + n = 1 \tag{4}$$

$$l + m\frac{f_1^2}{f_2^2} + n\frac{f_1^2}{f_3^2} = -\frac{\lambda_{abc}}{\lambda_1}(a + b\frac{f_1}{f_2} + c\frac{f_1}{f_3}) \tag{5}$$

The estimation cycle-slip value of combination observations can be calculated by Eq. (6) which is the time-differenced equation between two consequent epochs.

$$\Delta N = a\Delta N_1 + b\Delta N_2 + c\Delta N_3 = a\Delta\varphi_1 + b\Delta\varphi_2 + c\Delta\varphi_3 - \frac{(l\Delta P_1 + m\Delta P_2 + n\Delta P_3)}{\lambda} \tag{6}$$

For a, b and c and l, m and n can be calculated with two Eqs. (4) and (5). The combinations which is less affected by noise are selected. Suppose the noise of code is 0.3 m and phase is 0.01 cycle, some typical combinations are listed in the Table 1 [6].

According to Table 1, the GFIF combination (0, −1, 1) is the best one for BDS and (0, 1, −1) for GPS. Even the code noise is as large as 1 m, the value of combination cycle-slip can still be fixed at the success rate of 95.5% [1]. If there are no cycle-slips the value calculated by Eq. (6) is close to zero. However, only one GFIF is far not enough, because cycle-slip combinations cannot be detected by GFIF combinations, i.e. $\Delta N_1 = \Delta N_2 = \Delta N_3$, on the other hand, GFIF combinations are not able to calculate cycle-slips of individual frequency.

Table 1 Triple-frequency GFIF code-phase combination of GPS and BDS

	(*a*, *b*, *c*)	*l*	*m*	*n*	λ (m)	Standard error (cycle)
GPS	(0, 1, −1)	0.012109	0.444991	0.54290	5.8610	0.0533
	(1, −3, 2)	0.842594	0.15314	0.001092	1.2211	0.3033
	(1, −4, 3)	1.061142	0.080347	−0.141489	1.5424	0.3033
	(1, −2, 1)	0.699407	0.206086	0.094507	1.0105	0.3100
BDS	(a, b, c)	l	m	n	λ (m)	Standard error (cycle)
	(0, −1, 1)	0.019945	0.552577	0.427478	4.8842	0.0633
	(1, 1, −2)	0.750616	0.041406	0.207978	1.2967	0.2567
	(1, 3, −4)	1.577791	−0.537279	−0.040512	2.7646	0.2667
	(1, 0, −1)	0.597328	0.148645	0.254027	1.0247	0.2767

2.2 Phase Combinations

To enable the cycle-slips detection for each frequency, another two phase combinations are needed in addition to the GFIF combination (0, −1, 1) of BDS and (0, 1, −1) of GPS. Referred to [8], the geometric distance term in the phase combination observations could be eliminated by the GFIF combination with cycle-slips being repaired. The cycle-slip value of combination can be estimated using the epoch-differences [8].

For different combination observations, there exists relation as the Eqs. (7) shown:

$$\lambda_{a1b1c1}\Delta N_{a1b1c1} + \lambda_{a1b1c1}\Delta\varphi_{a1b1c1} + \beta_{a1b1c1}\Delta I_1 \approx \lambda_{a2b2c2}\Delta N_{a2b2c2} + \lambda_{a2b2c2}\Delta\varphi_{a2b2c2} + \beta_{a2b2c2}\Delta I_1 \quad (7)$$

$$\beta_{abc} = \frac{f_1^2(a/f_1 + b/f_2 + c/f_3)}{af_1 + bf_2 + cf_3} \quad (8)$$

where β_{abc} is the coefficient of phase combination (a, b, c); ΔI_1 in unite of meters is the ionospheric phase delay on the first frequency in cycles. Δ is the epoch-difference operator. The cycle-slip value of combinations can be estimated by Eq. (9).

$$\Delta N_{a1b1c1} \approx \frac{\lambda_{a2b2c2}\Delta N_{a2b2c2} - \lambda_{a1b1c1}\Delta\varphi_{a1b1c1} + \lambda_{a2b2c2}\Delta\varphi_{a2b2c2} + (\beta_{a2b2c2} - \beta_{a1b1c1})\Delta I_1}{\lambda_{a1b1c1}} \quad (9)$$

And the Eq. (10) is used in the detection of cycle-slip.

$$\Delta N_{a1b1c1} \approx \frac{\lambda_{a2b2c2}\Delta\varphi_{a2b2c2} - \lambda_{a1b1c1}\Delta\varphi_{a1b1c1} + (\beta_{a2b2c2} - \beta_{a1b1c1})\Delta I_1}{\lambda_{a1b1c1}} \quad (10)$$

At least 3 linear independence equations are needed for the detection and repair of cycle-slip. Equations can be formed as Eq. (10), with the appropriate coefficients. Supposing the pseudo-range noise is 0.3 m and the phase noise is 0.01 cycle. The criteria in coefficients selection is shown as following:

(1) If $\Delta I_1 = 0.5$ m, the noise of cycle-slip parameter ΔN_{a1b1c1} in Eq. (10) should be no more than 0.25 cycle. At this time, in the most of cases, the value of cycle-slip can be fixed at least at the success rate of 95.5% [8];
(2) The wavelength should be no less than 1 m in order to reduce the effect of ionospheric delay [9];

Table 2 The best combination coefficients of GPS and BDS

	Combination	The coefficients of phase combination (a, b, c)	The coefficients of code combination (l, m, n)	Threshold value
GPS	GFIF	(0, 1, −1)	(0.012109, 0.444991, 0.5429)	0.1800
	Phase combination 1	(1, −2, 1)		0.6300
	Phase combination 2	(−3, 3, 1)		0.3043
BDS	GFIF	(0, −1, 1)	(0.019945, 0.552577, 0.427478)	0.6636
	Phase combination 1	(1, 0, −1)		0.1553
	Phase combination 2	(−3, 2, 2)		1.0080

(3) The absolute value of the sum of combination coefficients should be no more than 1 and all combinations should be integer. In this case the ionospheric delay is reduced [1];
(4) The condition number of coefficients matrix composed by the coefficients of GFIF and phase combinations should be as small as possible.

Considering the signal feature of BDS and GPS, the coefficients can be searched in the range of [−10, 10]. The best coefficients is shown in the Table 2. If absolute value of cycle-slip parameter is larger than the threshold value, the cycle-slip is detected. All coefficients of three combinations is linear independence, when there is a cycle-slip in one frequency, the estimation of at least one combination cycle-slip value will be bigger than 1 cycle.

3 The Repair of Cycle-Slip

According to the relationship of combination ambiguity and ambiguity at each frequency, Eqs. (11) and (12) can be established. All coefficients are integer and $det(H) = \pm 1$, so each cycle-slip value can be calculated by $x = H^{-1}y$ which is more efficient compared with conventional searching method. Equation (11) is used for GPS and Eq. (12) is be used for BDS. The condition number of H in Eq. (11) is 44.9059, while the condition number of H in Eq. (12) is only 4.1982. From this point of view, the signal of BDS is better than GPS. When BDS-3 have been established, its signal will be different from BDS-2, the best combination need to be re-defined.

$$y = \begin{bmatrix} \delta N_{a1b1c1} \\ \delta N_{a2b2c2} \\ \delta N_{a3b3c3} \end{bmatrix} = \begin{bmatrix} 0 & 1 & -1 \\ 1 & -2 & 1 \\ -3 & 3 & 1 \end{bmatrix} \begin{bmatrix} \delta N_1 \\ \delta N_2 \\ \delta N_3 \end{bmatrix} = Hx \tag{11}$$

$$y = \begin{bmatrix} \delta N_{a1b1c1} \\ \delta N_{a2b2c2} \\ \delta N_{a3b3c3} \end{bmatrix} = \begin{bmatrix} 0 & -1 & 1 \\ 1 & 0 & 1 \\ -3 & 2 & 2 \end{bmatrix} \begin{bmatrix} \delta N_1 \\ \delta N_2 \\ \delta N_3 \end{bmatrix} = Hx \tag{12}$$

4 Data Processing and Analysis

The observation data of 1 s sampling rate of station WTZR (Germany) on the day of March 17, 2013 was used for validating of the model. Large magnetic storm happened on this day and TEC changed significantly over the equator, middle latitudes and auroral regions [6]. The data of GPS G24 phase data L1, L2, L5 and code data C1, C2, C5 were used from 15:00:00 to 20:00:00. Based on the file of ionosphere grid file of IGS on this day, with the calculation of GIM model, we found that TEC is large between 07:00:00 and 19:00:00. Therefore, this data could be used to check the capability of detection and repair of cycle-slips under the severe ionosphere environment. The second experiment is carried out using the 1 s sampling rate observations of station UNB3 (Canada) on March 13, 2016. BDS C12 is used include phase data L2, L6, L7 and code data C2, C6, C7 from 06:00:00 to 10:59:59. The third experiment used the data of AIRA (Japan) on August 17, 2017. The data of GPS G08 phase data L1, L2, L5 and code data Cl, C2, C5 were used from 00:00:00 to 04:59:59. For the data analysis, we used the software of Bernese 5.2 to detect the cycle-slips of the phase data of GPS G24, GPS G08 and no cycle-slip was found in the frequency of L1 and L2. Then we added cycle-slips in the phase data of GPS G24, GPS G08 and BDS C12 from the 5th epoch to 16875th epoch every 5 epochs, as followed: [0, 0, 1], [0, 0, 2],…,[14, 14, 15]. The number of manual-added cycle-slip was 3375.

4.1 Data Process

The calculation process is shown in Fig. 1. The first step is to read raw data and form combination observations. Secondly, cycle-slips are detected for current epoch. In the third step, the cycle-slips are determined and repaired in case that they exist. The process will be continued until the last epoch.

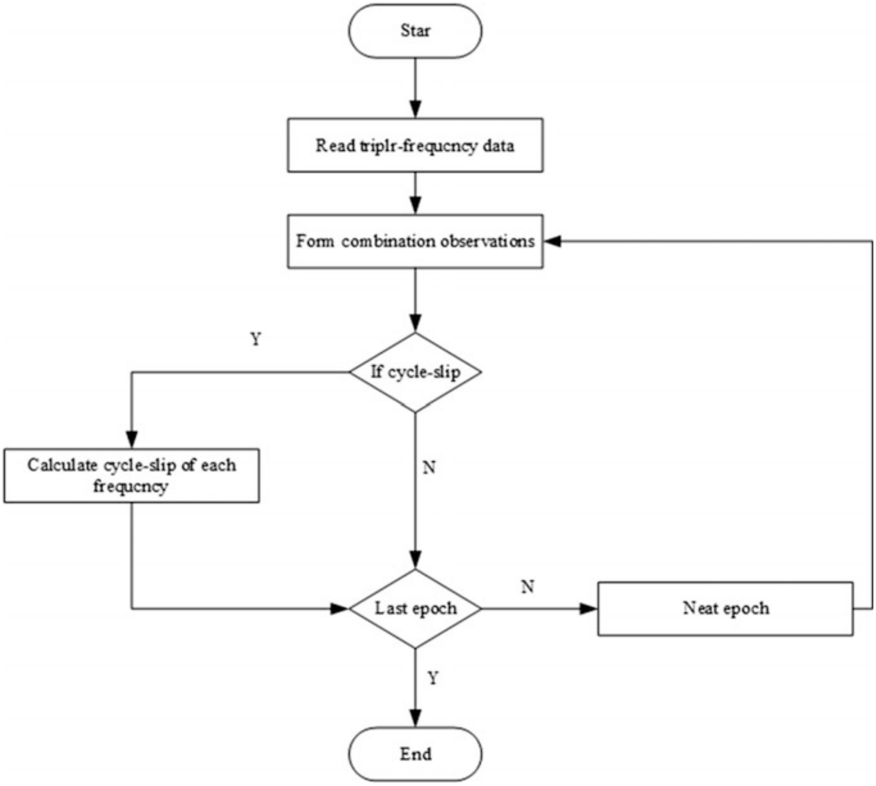

Fig. 1 Data processing flow chart

4.2 The Results of Cycle-Slip Detection and Repair

Based on the software of MATLAB 2016b and processor of CORE i3, taking the BDS data as an example, the processing time of cycle-slip detection and repair of 17,998 epochs data was 2.242 s, and the mean processing time for 1 epoch was around 125 microseconds. The cycle-slip parameters of GPS for the station WTZR are shown in Fig. 2 and BDS results for station UNB3, GPS results for AIRA are shown in Figs. 3 and 4. Shown in the figures all manual-added 3375 cycle-slips were precisely detected and repaired. Some of the results are shown in Tables 3, 4, and 5.

The difference the real and the fixed cycle-slip parameters of each frequency of station WTZR, UNB3 and AIRA are shown in Figs. 5, 6, and 7. As shown in the figures, the difference is between −0.5 cycle and 0.5 cycle for stations WTZR and UNB3. Due to poorer quality of the pseudo-range data of AIRA station, the difference is between −1.5 cycle and 1.5 cycle.

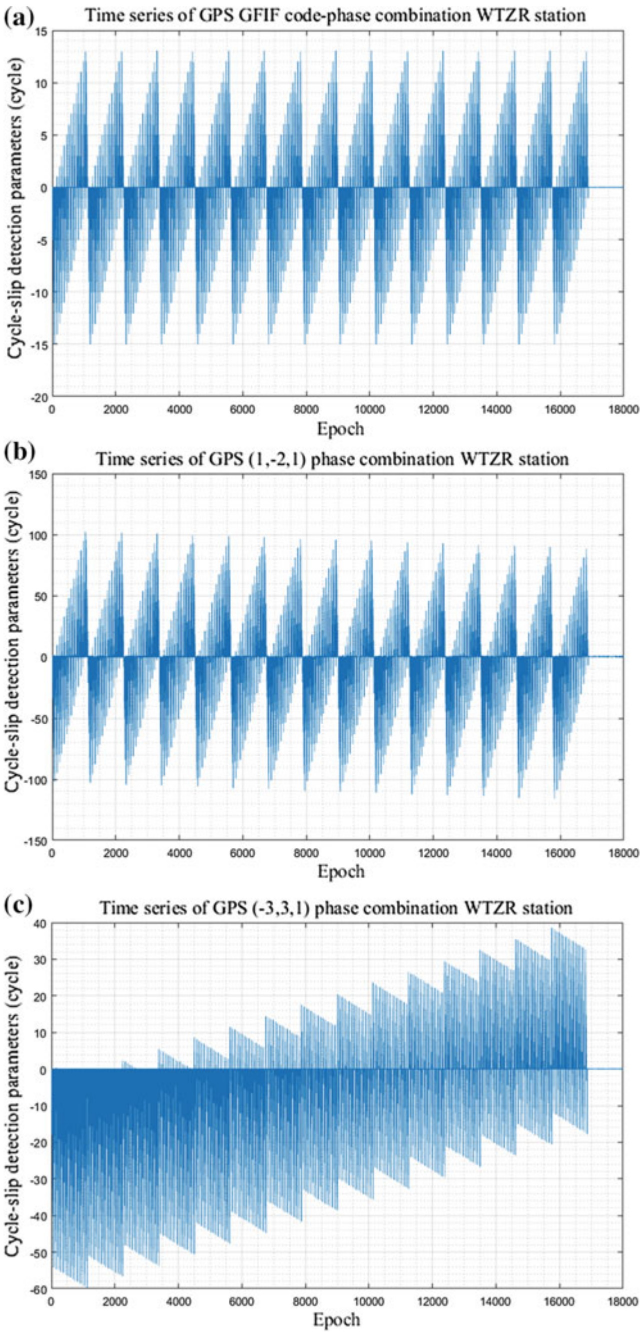

Fig. 2 Time series of all GPS cycle-slip detection parameters for station WTZR. **a** GFIF, **b** (1, −2, 1), **c** (−3, 3, 1)

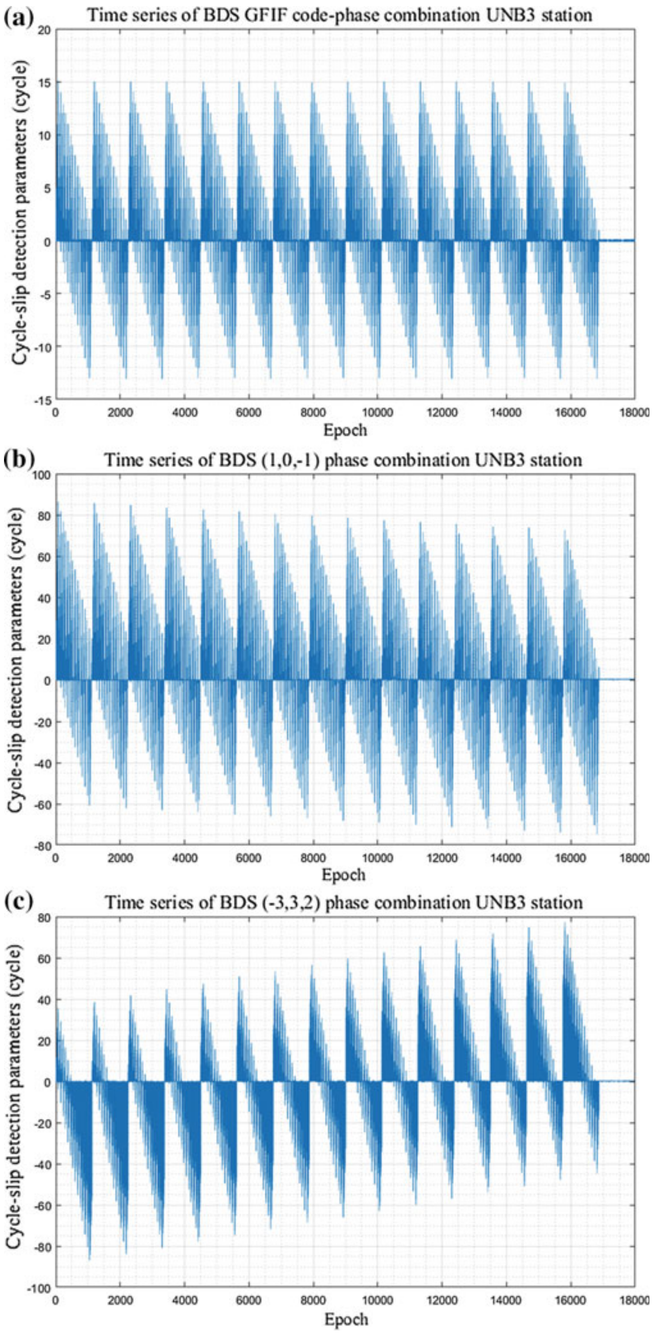

Fig. 3 Time series of all BDS cycle-slip detection parameters for station UNB3. **a** GFIF, **b** (1, 0, −1), **c** (–3, 3, 2)

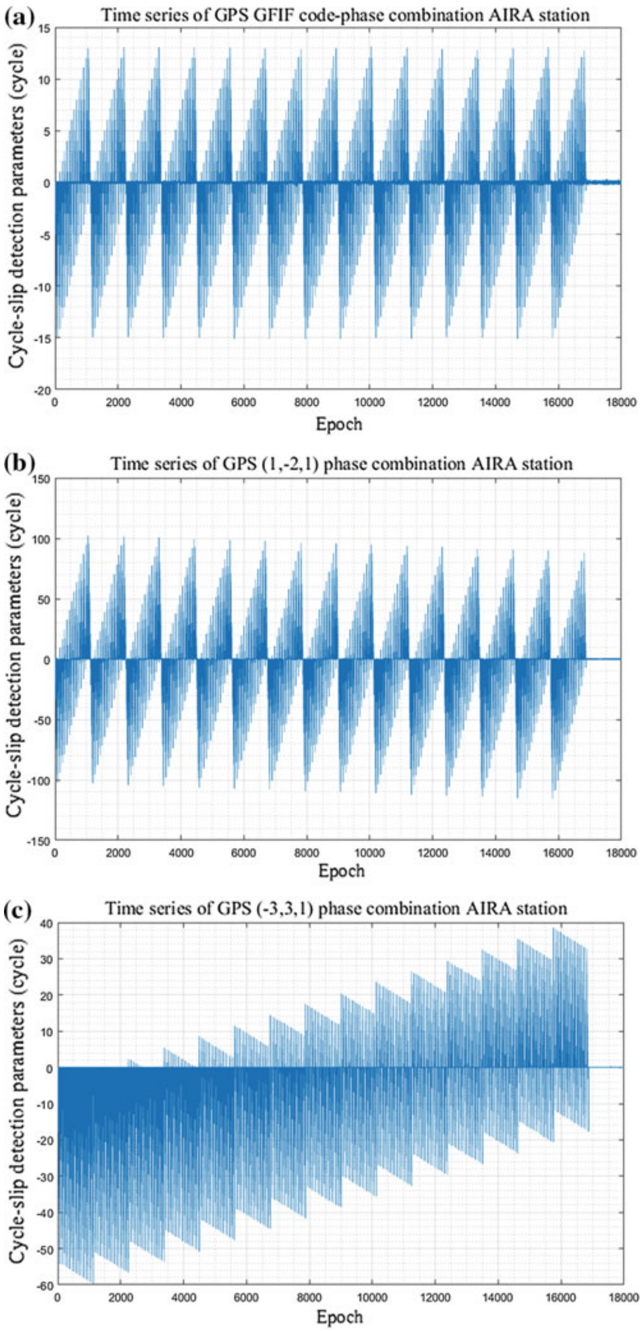

Fig. 4 Time series of all GPS cycle-slip detection parameters for station AIRA. **a** GFIF, **b** (1, −2, 1), **c** (−3, 3, 1)

Table 3 WTZR GPS G25 the results of cycle-slip detection and repair (parts)

Epoch	Point cycle-slip parameters (L1 L2 L5)			Fix cycle-slip parameters (L1 L2 L5)		
30	−0.1159	−0.0790	5.9244	0	0	6
35	−0.4539	−0.3446	6.6437	0	0	7
8035	6.9659	1.9737	1.9785	7	2	2
8040	7.1717	2.1321	3.1415	7	2	3
16,845	13.9789	13.9866	8.9826	14	14	9
16,850	14.0986	14.0757	10.0732	14	14	10

Table 4 UNB3 BDS C12 the results of cycle-slip detection and repair(parts)

Epoch	Point cycle-slip parameters (B1 B2 B3)			Fix cycle-slip parameters (B1 B2 B3)		
5	0.3963	0.3160	1.3399	0	0	1
10	−0.0485	−0.0272	1.9820	0	0	2
8010	6.7968	0.8418	11.8368	7	1	12
8015	7.1597	1.1206	13.1329	7	1	13
16,870	14.0817	14.0624	14.0607	14	14	14
16,875	14.3583	14.2758	15.2823	14	14	15

Table 5 AIRA GPS G08 the results of cycle-slip detection and repair(parts)

Epoch	Point cycle-slip parameters (L1 L2 L5)			Fix cycle-slip parameters (L1 L2 L5)		
20	−0.4265	−0.3127	3.6632	0	0	4
25	−0.3407	−0.2505	4.7544	0	0	5
8010	5.8949	0.1333	11.2570	7	1	12
8015	5.9712	0.2017	12.3046	7	1	13
16,840	15.0535	14.8138	8.7155	14	14	8
16,845	14.1006	14.0529	9.0651	14	14	9

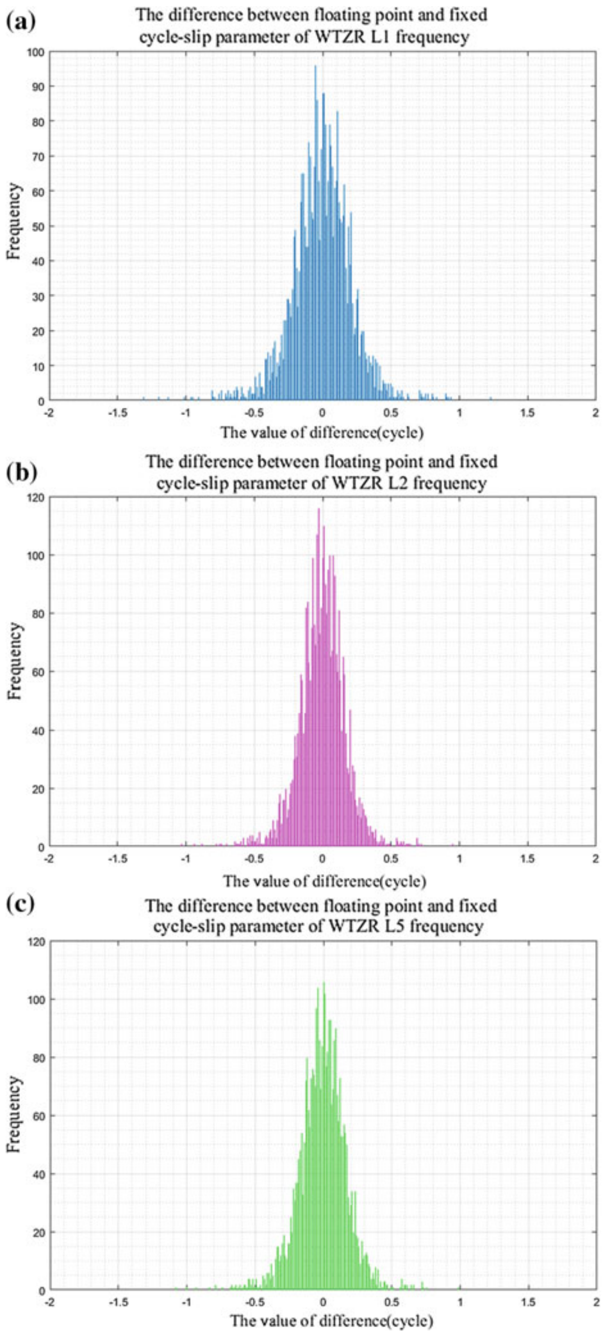

Fig. 5 The difference between the real and the fixed cycle-slip parameter of each frequency of WTZR station GPS G25. **a** L1, **b** L2, **c** L5

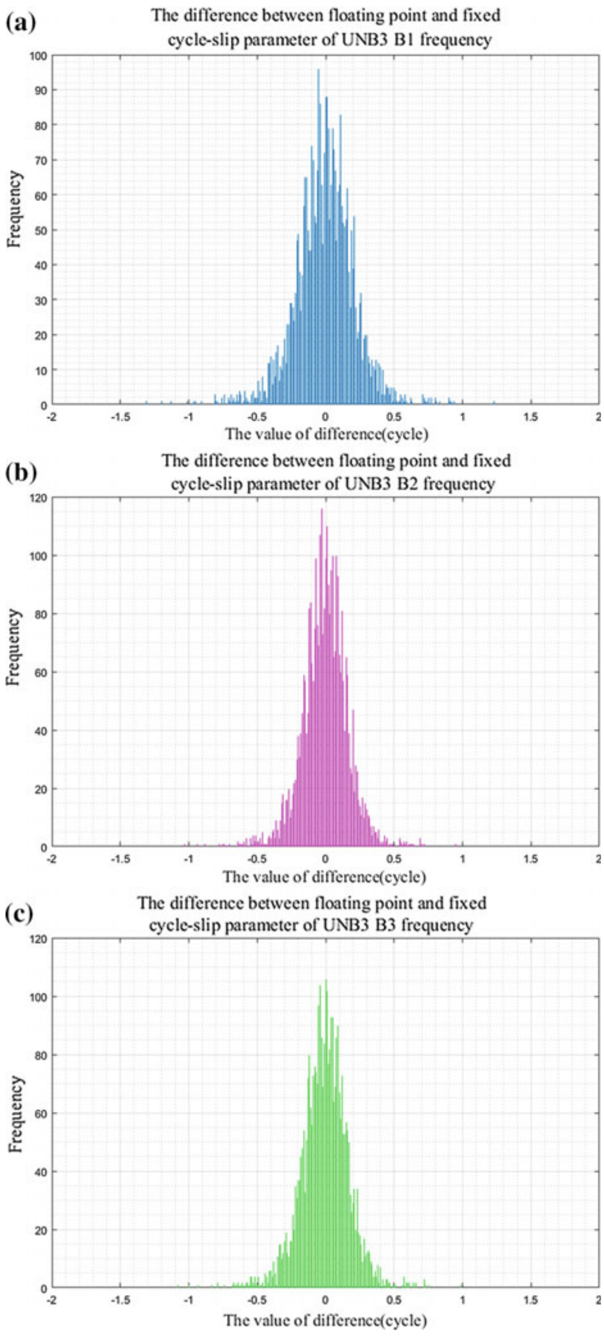

Fig. 6 The difference between the real and the fixed cycle-slip parameter of each frequency of UNB3 station BDS C12. **a** L2, **b** L6, **c** L7

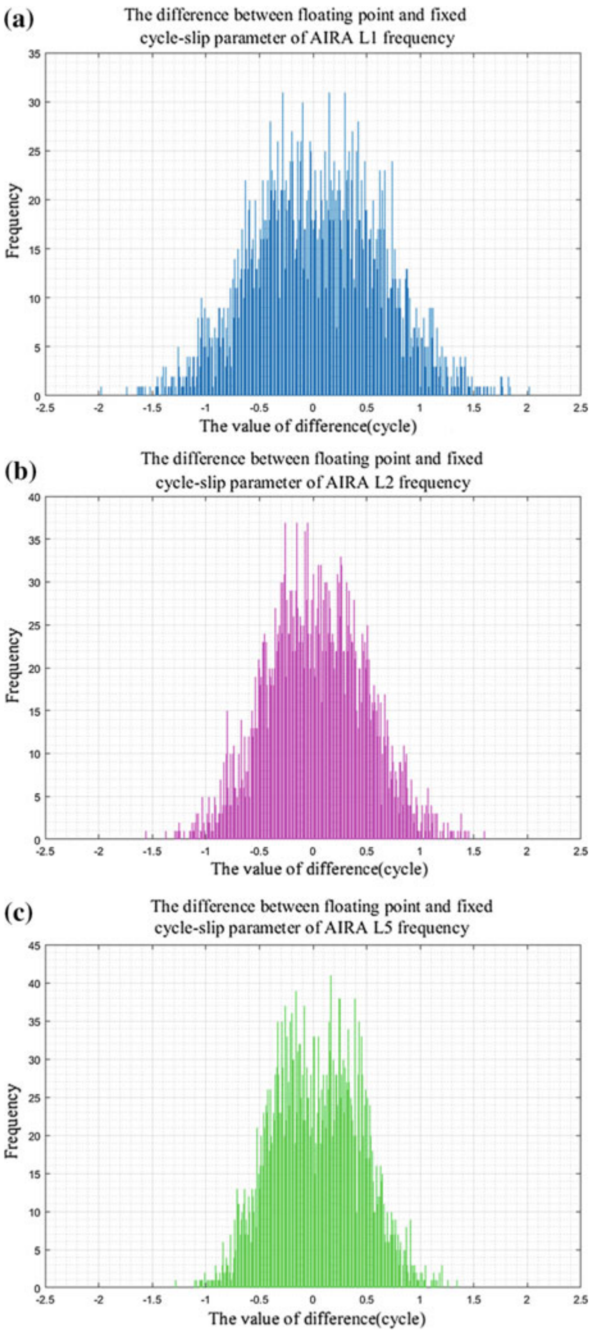

Fig. 7 The difference between the real and the fixed cycle-slip parameter of each frequency of AIRA station GPS G08. **a** L1, **b** L2, **c** L5

5 Conclusion

A more efficient method which is suitable for BDS and GPS for cycle-slip detection and repair is discussed in this paper. The cycle-slip parameters can be calculated without searching thus the efficiency is improved and stable. If some first epochs without cycle-slips or cycle-slips being repaired, using the method of phase smoothed pseudo-ranges can be applied to reduce the noise of pseudo-range and multipath. In addition, the results in the case of severe ionospheric delay with low sampling rate should be tested and the threshold value still can be optimized deeper.

Acknowledgements This work is support by the NSFC (No.11673050) and the 863 (No. 2014AA123102) projects.

References

1. Li J, Yang Y et al (2011) Real-time cycle-slip detection and repair based on code-phase combination for GNSS triple-frequency un-differenced observations. J Acta Geodaetica Cartogr Sin 40(6):717–722
2. Feng YM (2008) GNSS three carrier ambiguity resolution using ionosphere-reduced virtual signals. J Geodesy. https://doi.org/10.1007/s00190-008-0209-x
3. Zhang Y (2017) Research on real-time high precision BeiDou positioning service system. Tongji University, Shanghai
4. Li Z, Huang J (2016) GPS surveying and data processing. Wuhan University Press, Wuhan
5. Wang C, Wang J (2012) Cycle slip detection and correction of single-frequency undifferenced phase observation. J Tongji Univ (Natural Science). https://doi.org/10.3969/j.issn.0253-374x.2012.09.020
6. Huang L, Zhai G, Ouyang Y et al (2015) Triple-frequency TurboEdit cycle-slip processing method of weakening ionospheric activity. J Acta Geodaetica et Cartographica Sinica. https://doi.org/10.11947/j.AGCS.2015.20140380
7. Wang X, Wen Xiang LIU et al (2016) Detection and repair of cycle-slip for undifferenced BDS triple-frequency observations. J Nat Univ Defense Technol. https://doi.org/10.11887/j.cn.201603003
8. Wang X (2016) Research on high precision positioning data processing technology of Beidou satellite navigation system. National University of Defense Technology, Changsha
9. Yao Y, Gao J et al (2014) Real-time cycle-slip detection and repair for compass triple-frequency carrier pahse observations. J China Univ Minimaling Technol. https://doi.org/10.13247/j.cnki.jcumt.000242